OTC 23811

An Improved Method of Extremal Value Analysis of Arctic Sea Ice Thickness Derived From Upward Looking Sonar Ice Data

E. Ross, D. Fissel, J. Marko, J. Reitsma, ASL Environmental Sciences Inc.

Abstract

In the Beaufort Sea, observations of extreme draft sea ice features have been identified from upward looking sonar (ULS) datasets spanning several years. Using analysis methods from extreme value theory, the estimated 100-year return values of the maximum ice draft have been derived. In addition, the applicability of these statistical techniques to the Northeast Greenland ice regime is examined using one year of ULS data at two locations from 2008 to 2009.

The methods have been developed for the Beaufort Sea region and subsequently, further refined for use in estimating extreme ice hazards off Northeast Greenland. These estimates provide inputs to the design of offshore platforms and ships in support of oil and gas activities in these ice-infested waters.

Previous studies in the Canadian Beaufort Sea derived an empirical upper limit on the maximum sea ice thickness resulting from deformation processes based on the relationship of maximum ice thickness as a function of simultaneous values of undeformed ice thickness. Using the more extensive ULS ice keel data sets now available, these methods were re-evaluated and updated. Similar analyses were carried out on ice thickness measurements obtained off Northeast Greenland which reveal distinct differences in the ice regime of these two geographical areas.

Improvements to extremal value statistical analysis methods for long recurrence intervals of 100 years for ice draft (D_{100}) are based on the three parameter Weibull distribution which has been optimized for application to very large sea ice keels using a peak over threshold selection approach. These results were compared to the maximum draft limit and undeformed ice thickness relationship. We developed techniques to refine at a high resolution the lower threshold on maximum draft and examine the implications of this filtering on D_{100}. This is an important consideration as selecting the lower maximum draft threshold is a balance between retaining enough observations to ensure statistical robustness and sampling only the extreme tail of the maximum draft distribution. Methods for performing these statistical analyses are presented.

Introduction

Commercial and industrial activities in the Arctic and other ice-infested waters experience unique operational conditions. In particular, offshore vessels and structures must be designed to withstand ice loads including the sustained internal pressure within an ice field and the complex interactions with individual ice features. Ice management provides another strategy to mitigate the operational impact of ice loads although this approach may not be sufficient in the most extreme load conditions [1].

An input to any ice load mitigation strategy must include an estimate of the extreme ice drafts expected in a region of interest. The undersurface of sea-ice is highly variable and physical mechanisms which produce the extreme keels may occur far from the region of interest. These characteristics of ice topography and dynamics suggest that there is a reduced likelihood of directly observing the extreme of the ice draft distribution for a region; however, with a large enough sample population it is possible to estimate 100-year return values for the ice keel maximum draft using observations of individual ice keels.

Upward looking sonar (ULS) instruments have been used for two decades to provide time-series observations of ice draft in ice-infested areas [2]. Ice draft is determined with high temporal resolution (measurements

typically at 1-2 second intervals) and spatial resolution (typically 0.05 m accuracy). Continuous sampling for over a year provides a long time-series containing typically hundreds or thousands of individual ice keel features. Other ULS instruments are used concurrently to measure ice velocity and are integrated with the ice draft data to provide a measure of the horizontal extent of ice features.

The generation of ice features with significant draft is driven by deformation of relatively level ice which has grown thermodynamically. The largest amount of deformation within this level ice is caused by the relative motion of neighbouring ice sheets. The level ice undergoes mechanical failure and is deformed into a pressure ridge. This process transforms ice which is less than a few metres thick into keel features which can be several tens of metres in draft.

In shallower waters, the water depth may provide a limiting factor on the maximum possible keel draft. However, in deeper waters, there is a finite probability that the maximum possible keel draft generated by deformation processes involving level ice would pass by a specific location in a given time period. Extreme value theory provides the methods to determine this probability and effectively estimate the expected extreme maximum keel draft in a region based on numerous keel draft samples from that region.

The connection between level ice and deformed ice through physical processes suggests a possible relationship between the draft of deformed ice features and the draft of the level ice involved in the deformation processes. Amundrud et al. [3] investigated this concept using ice draft observations in the Beaufort Sea acquired in the 1990s and found an empirical relationship between keel draft, d, and level ice draft, h, where these parameters are expressed in units of metres:

$$d = 20h^{1/2} \qquad (1)$$

Ice Draft Measurement

ASL's Ice Profiler (IPS) provides measurments of ice draft and has been used in many ice-infested areas [4]. The operation of the IPS is depicted in Figure 1. The instrument determines the time-of-flight for the travel of short acoustic pulses from the instrument to a water column target and back to the instrument. The range of the target from the instrument is then calculated using the speed of sound through the water column. A single ping may determine the range to multiple targets. The latest version of the IPS is capable of storing up to five targets per ping and the full profile of the backscattered returns.

Additional measurements by the IPS of the instrument tilt and depth enable conversions of the range measurements to target draft, d, through:

$$d = \eta - \beta \cdot r \cdot \cos\theta \qquad (2)$$

where r is the range to a target, θ is the total instrument tilt and β is a time-dependent correction factor which scales range for variations in the speed of sound. This correction factor is empirically determined by identifying episodes of open water which, by definition, have zero draft allowing β to be determined from Equation 2 as:

$$\beta = \frac{\eta}{r \cdot \cos\theta} \qquad (3)$$

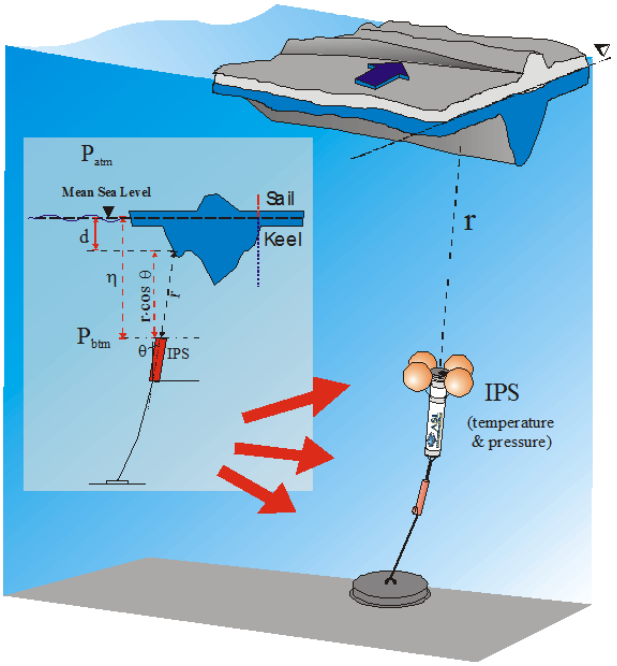

Figure 1: The ASL Ice Profiler (IPS) measures the profile of the ice undersurface along the direction of ice drift.

The IPS is deployed to transmit pings typically at 1-2 second intervals. This leads to a high-resolution profile of the ice undersurface as depicted in Figure 2 with ice drafts accurate to about 0.05 m.

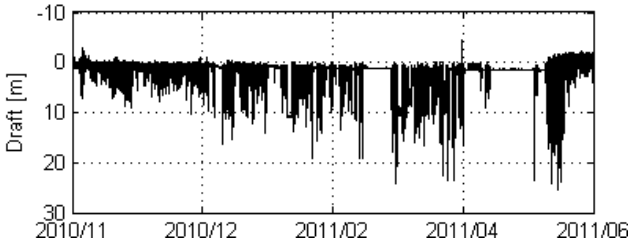

Figure 2: Time-series of ice draft measurements in the Beaufort Sea from Nov 2010 to Jun 2011.

The ice draft time-series is subsequently transformed to an equispaced distance interval by integration with ice velocity measurements obtained by an Acoustic Doppler Current Profiler (ADCP) co-deployed within 100 m. An example of the final ice draft evenly spaced in distance is shown in Figure 3 for a short segment.

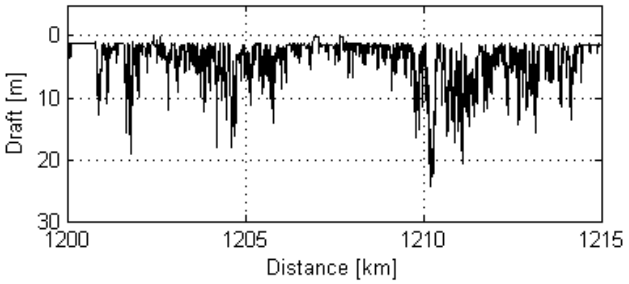

Figure 3: Ice draft measurements from the Beaufort Sea transformed to an evenly spaced distance interval determined from measurements of ice velocity.

The data used in our analysis was obtained in two locations in the Beaufort Sea and two locations off Northeast Greenland in Fram Strait (Table 1).

Table 1: The ASL Ice Profiler deployments used in this study.

Region	Site	Number of years	Location
Beaufort Sea	1	9	70.33°N / 133.74°W
	2	7	70.99°N / 133.75°W
Fram Strait	1	1	78.85°N / 5.35°W
	2	1	78.82°N / 6.44°W

Ice Keel Identification

A feature detection algorithm was used to identify individual keel features within an equispaced ice draft series. Three parameters characterize the algorithm:

- **Start threshold** – The draft value which triggers the identification of an ice keel. Forward and backward searches for the end and start of the keel, respectively, are performed from the draft data record that exceeds the start threshold.
- **End threshold** – The absolute minimum draft value which triggers the boundary of a keel, i.e. the start or end. This is typically set to the expected level ice draft in the region of interest determined through ice charts and ice draft time-series.
- **Alpha** – The Rayleigh criterion which is used to determine an adaptive draft threshold for detecting the start or end of a keel. The draft threshold, d_T, based on this parameter is calculated as:

$$d_T = (1 - \alpha) d_{max} \quad (4)$$

where d_{max} is the maximum of the draft records that comprise the keel feature.

The draft data is scanned from the beginning until a draft record exceeds the start threshold. This point establishes the current start of an individual keel. The draft data is scanned from the start of the keel while continually updating d_{max} and checking if the keel has ended by a draft record that is either (1) less than the end threshold or (2) less than the adaptive draft threshold and the slope has reversed. Upon finding the end of the keel, the start of the keel is found by searching backward from the current start using the same criteria as was used to find the keel end. The maximum keel draft is not updated during the backwards scan. The search results in a list of start and end record indices that identify individual keel features from the complete draft data (Figure 4).

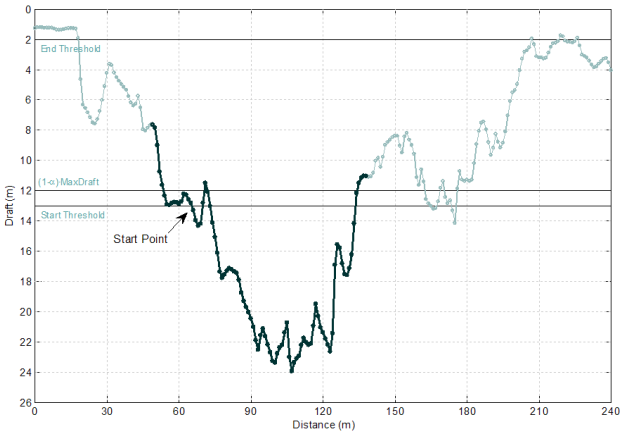

Figure 4: An example of the thresholds used by the keel feature detection algorithm. This particular keel was found using a 13 m start threshold, 2 m end threshold and α equal to 0.5.

After identifying the start and end record indices of all qualifying keel features, features that overlap are combined into a single keel (Figure 5). Overlaps can occur due to the changing impact of the adaptive draft threshold on the start and end points.

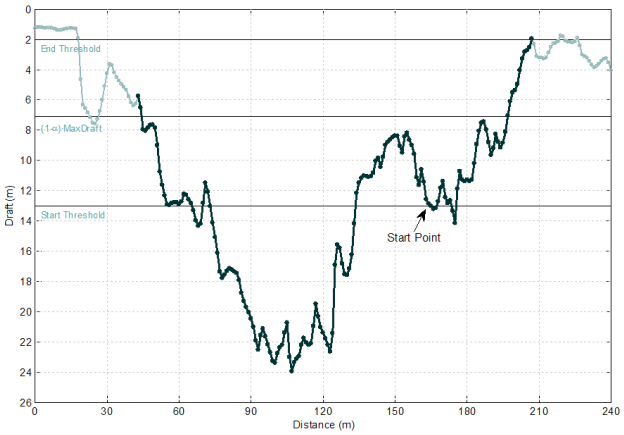

Figure 5: An example of the keel from Figure 4 that has been combined with its neighbouring and overlapping keel features.

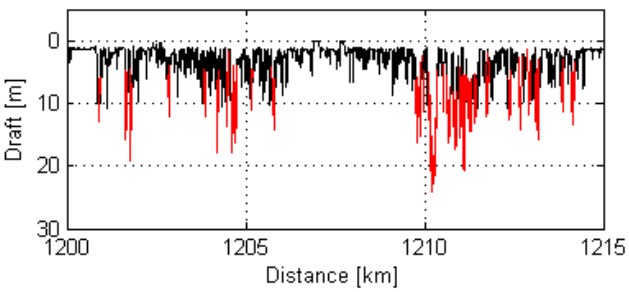

Figure 6: Ice draft measurements from the Beaufort Sea transformed to an evenly spaced distance interval with keel features identified (red).

In our analysis we used an end threshold of 2 m and a value for α of 0.5. Since we are concerned with the extreme end of the keel draft distribution we used a start threshold of 11 m. Applying the keel detection algorithm with the stated parameter values to the ice draft data plotted in Figure 3 results in the keels identified in Figure 6.

Level Ice and Maximum Keel Draft

An analysis by Amundrud et al. [3] led to an empirically determined relationship between the maximum ice draft and the draft of nearby level ice based on draft observations from the Beaufort Sea in the 1990s. They argued that ridging in first-year ice continues as long as the force required to drive an ice block over the ridge is less than the force at which the level ice next to the ridge will buckle.

We performed a similar empirical analysis on recent draft observations from the Beaufort Sea and Fram Strait. The equispaced ice draft records at two locations for these years were divided into 50 km segments. For each segment the following procedure was used:

- The maximum draft of each segment was found and its distance location was recorded.
- The draft data within 5 km of the maximum draft was extracted.
- A histogram of the extracted draft data segment was calculated using 0.2 m bins.
- The mode of the draft distribution was found by selecting the bin containing the maximum number of data values.
- The median of the data values in the selected bin and its two neighbouring bins was calculated and this was determined to be the level ice draft in the region of the maximum draft event.

An example of this process is shown in Figure 7. The 50 km draft segment is plotted in grey with the 5 km sub-segment of draft values about the maximum draft shown with black markers. The histogram of the draft values in the sub-segment is shown on the right. The level ice draft derived from the median of the data values in the bin corresponding to the maximum of the histogram is shown plotted in red.

The draft data from the two locations in the Beaufort Sea spanned 1999 to 2011 and produced 699 segments of 50 km of ice draft. Figure 8 shows a comparison of the maximum keel drafts and their associated level ice drafts. The maximum ice draft truncation curve determined by Amundrud et al. (Equation 1) is also shown for comparison. The curve represents a reasonable bound on the limiting maximum ice draft generated from level ice.

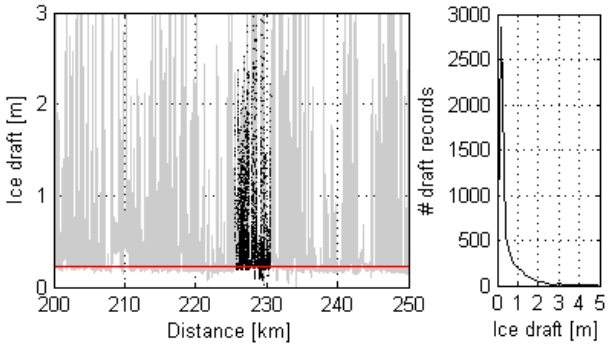

Figure 7: An example of the determination of the level ice draft (red) in the segment of data near the maximum draft (black) of a 50 km segment of equispaced ice draft (grey). The righthand plot shows the draft distribution of the black data values.

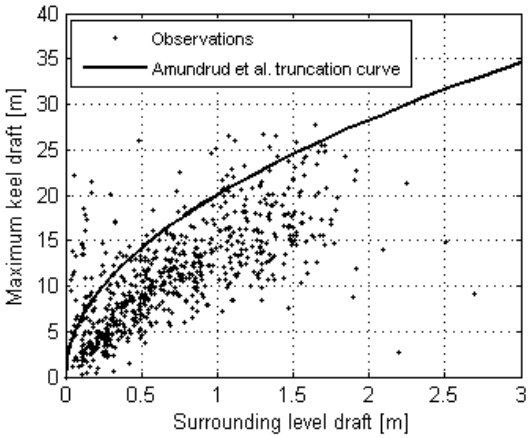

Figure 8: The maximum ice draft truncation curve realized from draft observations made at two locations in the Beaufort Sea from 1999 to 2011.

As with the Amundrud et al. results, there are many values that exceed the truncation curve, which is attributed to pinnacles on keels or a refrozen crack near the ridge. Eleven percent of our results fall in this category compared to less than four percent in the Amundrud et al. results. Some differences are expected as they filtered ridges generated from multi-year ice while we did not. Current work is underway to improve the automatic identification of multi-year ice in IPS data. If these features could be filtered from our results, it is expected that few observations would remain above the truncation curve in Figure 8.

Although only two deployment-years of ice draft data were used in the analysis of Fram Strait (two locations for one year each), this resulted in 238 segments of 50 km of ice draft. This compares to the 699 segments analyzed for the Beaufort Sea data across the 16 deployment-years.

Figure 9 shows the analysis results for the Fram Strait ice draft data and there is a clear difference from the Beaufort Sea results. The extracted maximum draft values and their corresponding surrounding level draft appear to divide into two clusters. Most of the lefthand cluster lies above the Amundrud et al. truncation curve and may, as with the Beaufort results, correspond to features generated

by ridging involving multi-year ice. Some points within this cluster lie on the truncation curve. The other cluster lies almost entirely below the truncation curve.

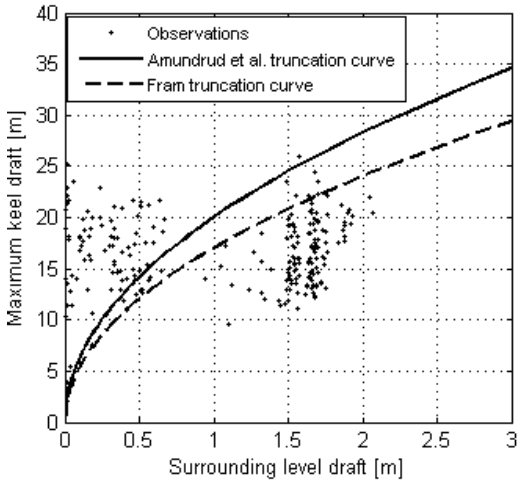

Figure 9: A regional maximum ice draft truncation curve (dashed) realized from draft observations made at two locations in Fram Strait from 2008 to 2009. The Amundrud et al. truncation curve (solid) based on Beaufort Sea observations is shown for comparison.

Another truncation curve which is perhaps more appropriate for the Fram Strait results is shown as a dashed line. This truncation curve is given by:

$$d = 17h^{1/2} \qquad (5)$$

The Fram Strait draft distribution of the 5 km segments that surrounded the maximum draft events were strongly bimodal. This most likely caused misidentifications of the level ice draft. Further refinement of the algorithm is necessary to localize the level ice draft most relevant to a maximum ice draft event. Another possibility is to shorten the segment over which the equispaced draft data is divided in order to statistically reduce the effect of misidentification.

Extreme Ice Draft

The keel detection algorithm described above was used to detect individual keel features that exceed 11 m in maximum ice draft. This resulted in thousands of identified features as listed in Table 2. The exceedance distribution of these keels by maximum draft normalized by the number of years over which they were observed is shown in Figure 10. The identified keels are further filtered by setting a draft threshold to obtain only those keels in the high end of the draft distribution.

Table 2: The number of keels identified at each site for the Beaufort Sea and Fram Strait locations.

Region	Number of identified keels (site-years)		
	Site 1	Site 2	Total
Beaufort Sea	2621 (9)	1818 (7)	4439 (16)
Fram Strait	1213 (1)	2224 (1)	3437 (2)

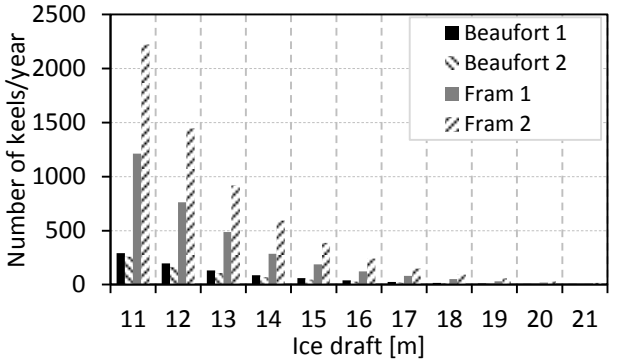

Figure 10: Maximum keel draft exceedance distributions for the four measurement locations over all site-years.

Estimates of keel depth values that, on average, would be expected to be exceeded at a given site within 100 years, D_{100}, are derived by fitting the high ice draft end of the empirical keel probabilities to the three-parameter Weibull probability distribution, which is one of the few distributions frequently used in extreme value analyses. When written in terms of the exceedance probability, $E(x)$, for maximum draft values greater than value x, this distribution can be written as:

$$E(x) = 1 - e^{-\left(\frac{x-\mu}{a}\right)^b} \qquad (6)$$

Determinations of the scale parameter a, the shape parameter b and the location parameter μ which optimize the fit of Equation 6 to empirical cumulative probabilities for individual keel draft values allow the computation of D_{100}. In practice, if N keels are included in the development of the empirical cumulative probability distribution for S sites, and Y_j individual years at each site, this critical exceedance is given by:

$$E(D_{100}) = \frac{\sum_{j=1}^{S} Y_j}{100N} \qquad (7)$$

The value of x for which the optimized version of Equation 6 becomes equal to Equation 7 yields an estimate of D_{100}.

Empirical values of exceedance as a function of lesser draft values are expressed as $E(D_i)$, where D_i is the ith keel draft value and i denotes the index of this draft value in an ascending order list of the maximum drafts of all keels used in the study:

$$E(D_i) = 1 - \frac{i}{N+1} \qquad (8)$$

Our procedure carries out maximum likelihood calculations for the parameters a and b in Equation 6 which minimize differences between the fitting function, Equation 6, and the measured empirical exceedances, $E(D_i)$, for values of μ incremented and decremented in 0.01 m steps about the lowest draft value used in obtaining our empirical estimates of $E(D_{100})$. Equation 7 can be used to obtain empirical exceedance estimates based upon composite sets of data collected during the several years included the analysis.

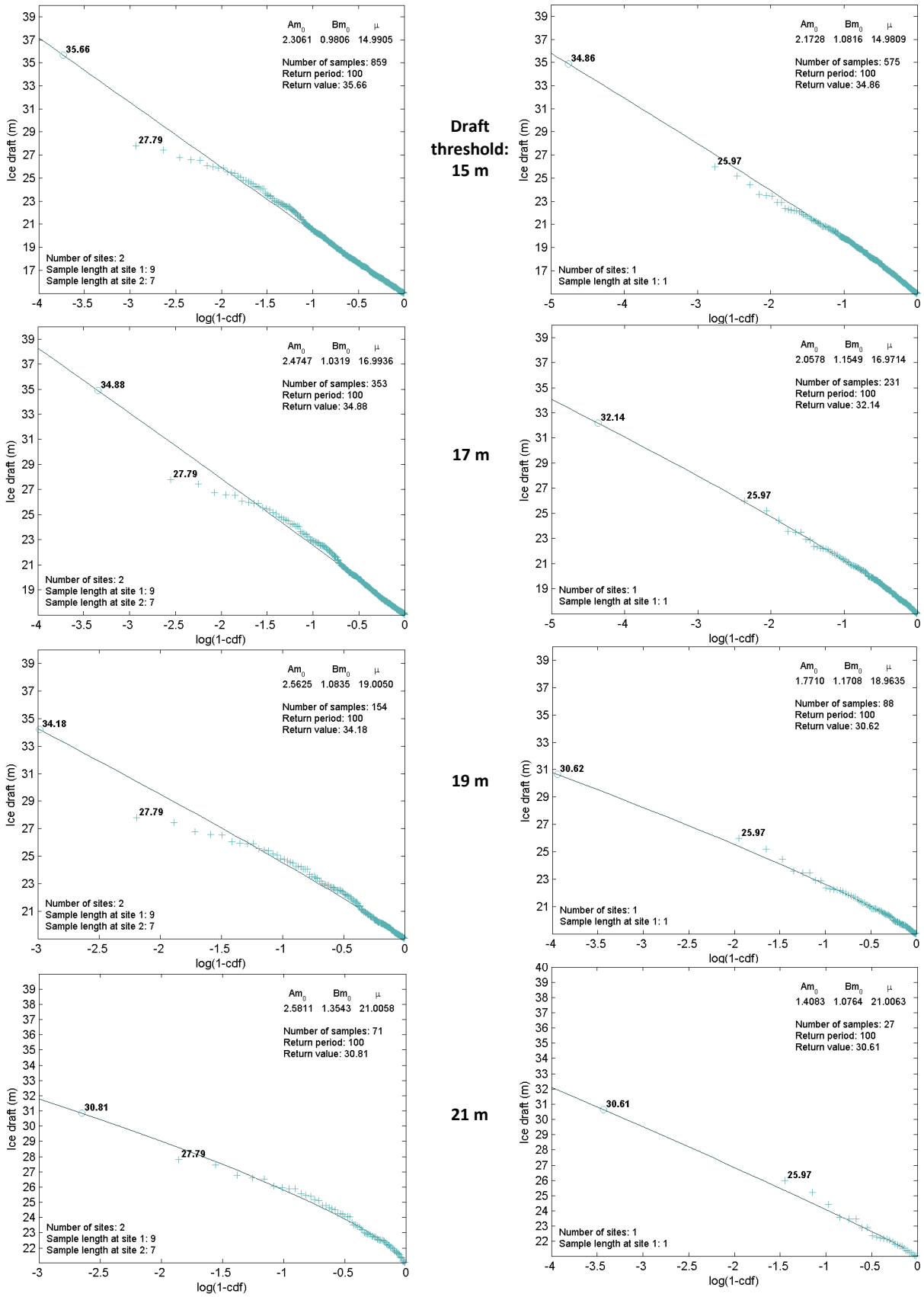

Figure 11: Fits of the three parameter Weibull cumulative distribution function for the combination of both Beaufort Sea sites (left column) and both Fram Strait sites (right column). The maximum keel draft observations used to perform each fit are truncated using varying draft thresholds from top to bottom of 15, 17, 19 and 21 m.

Qualitative assessments of the Weibull distribution fits for various draft thresholds can be obtained via the plots shown in Figure 11. These plots show the curve based on the optimized three parameter Weibull distribution and the keel feature maximum draft values used in the fit. The results based on various draft threshold (15, 17, 19 and 21 m) are shown to illustrate the sensitivity of D_{100} to the draft threshold. An initial assessment of the Beaufort Sea results suggest that the 21 m threshold produces a good fit. The plots for the Fram Strait data are not as definitive in their results.

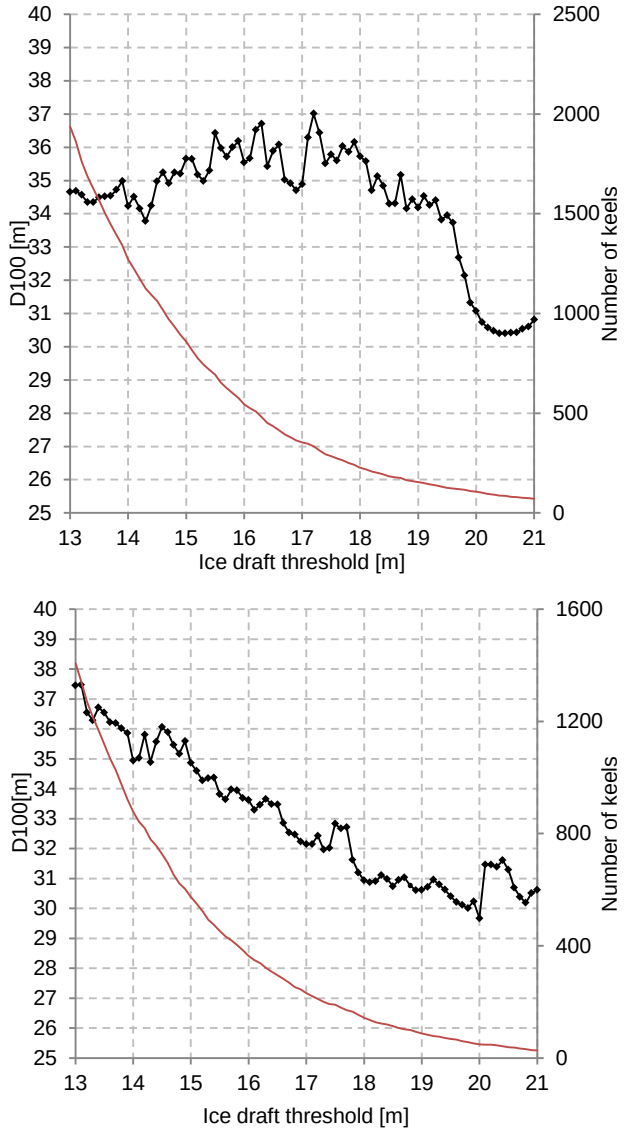

Figure 12: 100-year return value (black) of maximum keel draft for varying draft threshold used in filtering the keel population for the Beaufort Sea (top) and Fram Strait (bottom). The red line shows the number of keels used in determining each D_{100} value.

It appears from the plot based on the Beaufort Sea 15 m draft threshold result that the fitted data may contain maximum draft values that do not lie in the extreme of the keel maximum draft distribution. Selection of the draft threshold to filter these keel drafts is a delicate exercise as the keel population decreases rapidly with increasing draft threshold. A threshold that is at or near the extreme of the distribution tail while leading to a significant population size is ideal.

In order to fine-tune the draft threshold to balance these needs, we varied the threshold in steps of 0.1 m from 13 m to 21 m and determined the resulting D_{100} at each step. Plots of the response of D_{100} with draft threshold are shown in Figure 12. These curves tend to consist of relatively stable regions separated by episodes with high gradient. The Beaufort Sea curve shows two stable levels of D_{100} at about 35 m and 31 m. The Fram Strait curve suggests a possible stable level of D_{100} at about 31 m.

The underlying mechanisms that lead to the typical form of the D_{100} response to draft threshold are not fully understood. The levels of D_{100} values that are relatively stable may represent different dominating deformation mechanisms or geographically different sources of extremely deformed keels. In any case, these curves help constrain the likely range of D_{100} values.

Conclusions

An empirical relationship of maximum ice draft to nearby level ice draft was determined using recent data from the Beaufort Sea. This relationship was found to agree with previous estimates of $20h^{1/2}$. The same analysis applied to data obtained from Fram Strait suggests a relationship with a smaller scaling factor, i.e. $17h^{1/2}$. It is important to note that this relationship is based on results which may include several anomalous segments. Further work is necessary to remove or reduce the impact of these segments on the relationship.

Extreme value analysis applied to the maximum drafts of individually identified keels suggests that the 100-year return value for the maximum keel draft at the Beaufort Sea locations is about 32±2 m and at the Fram Strait locations is about 33±4 m; however, additional data is needed at the Fram Strait to expand the statistically limited two site-year database.

The above 100-year return value estimates for maximum draft agree with the values determined by the regional truncation curves to within 20% (28 m based on a 2 m level ice draft for the Beaufort Sea and 29 m based on a 3 m level ice draft for Fram Strait).

References

1.Eik, K., *Sea-ice management and its impact on the design of offshore structures.* Cold Regions Science and Technology, 2011. **65**(2): p. 172-183.

2.Fissel, D.B., J.R. Marko, and H. Melling. *Advances in Marine Ice Profiling for Oil and Gas Applications*. in *Icetech*. 2008. Banff, Alberta, Canada.

3.Amundrud, T.L., *Geometrical constraints on the evolution of ridged sea ice.* Journal of Geophysical Research, 2004. **109**(C6).
4.Fissel, D.B., et al. *Automated Detection of Hazardous Sea Ice Features from Upward Looking Sonar Data*. in *Icetech*. 2010. Anchorage, Alaska, USA.